

Space- and time-resolved observation of extreme laser frequency upshifting during ultrafast-ionization

A. Giulietti,^{1,a)} A. André,² S. Dobosz Dufrénoy,² D. Giulietti,^{1,3,4} T. Hosokai,⁵ P. Koester,¹ H. Kotaki,⁶ L. Labate,^{1,4} T. Levato,¹ R. Nuter,^{7,b)} N. C. Pathak,^{1,c)} P. Monot,² and L. A. Gizzi^{1,4}

¹*Intense Laser Irradiation Laboratory, Istituto Nazionale di Ottica, CNR Campus, Via Moruzzi, 1, 56124 Pisa, Italy*

²*CEA-Saclay DSM-IRAMIS-SPAM, 91191 Gif sur Yvette, France*

³*Dipartimento di Fisica, Università di Pisa, Pisa, Italy*

⁴*Istituto Nazionale di Fisica Nucleare, Pisa, Italy*

⁵*Photon Pioneer Center, Osaka University, Osaka, Japan*

⁶*Japan Atomic Energy Agency (JAEA), Kizugawa, Kyoto, Japan*

⁷*CEA-Arpajon DIF-DAM, Arpajon, France*

(Received 16 April 2013; accepted 29 July 2013; published online 20 August 2013)

A 65-fs, 800-nm, 2-TW laser pulse propagating through a nitrogen gas jet has been experimentally studied by 90° Thomson scattering. Time-integrated spectra of scattered light show unprecedented broadening towards the blue which exceeds 300 nm. Images of the scattering region provide for the first time a space- and time-resolved description of the process leading quite regularly to such a large upshift. The mean shifting rate was as high as $\delta\lambda/\delta t \approx 3 \text{ \AA}/\text{fs}$, never observed before. Interferometry shows that it occurs after partial laser defocusing. Numerical simulations prove that such an upshift is consistent with a laser-gas late interaction, when laser intensity has decreased well below relativistic values ($a_0 \ll 1$) and ionization process involves most of the laser pulse. This kind of interaction makes spectral tuning of ultrashort intense laser pulses possible in a large spectral range. © 2013 AIP Publishing LLC. [<http://dx.doi.org/10.1063/1.4818602>]

I. INTRODUCTION

Spectral changes of intense light pulses propagating in a medium have been studied since high power pulsed lasers came into play.^{1–4} After the introduction of chirped pulse amplification (CPA) laser technology,⁵ investigations extended to ultrashort laser pulses propagating in plasmas.^{6,7} In particular, Le Blanc *et al.*⁶ reported one of the first clear observations of spectral blue shifting of a femtosecond laser pulse propagating in a dense gas. Interestingly, a well defined spectral shift was also measured after anomalous propagation in an overdense plasma slab.⁸ A number of papers report on spectral effects in conditions of interest for laser driven electron acceleration. Koga *et al.*⁹ observed blue shift up to 40–50 nm, which was attributed to a combined effect of ionization and filamentation. Giulietti *et al.*¹⁰ observed 25 nm peak blue shift with modulated spectral tails extending up to 100 nm, mostly attributed to self-phase modulation. Murphy *et al.*¹¹ observed both red and blue shifts, attributed to "photon acceleration" with "wake signature" in the red side of the spectrum. Trines *et al.*¹² observed both red and blue shifts but blue shift was dominant and showed modulations, which were attributed to wake-driven photon acceleration and modulational instability. Thomas *et al.*¹³ analyzed spatially resolved spectra of laser light scattered sideward from a laser-driven electron accelerator. Operating

at relativistic intensity, they found that Raman scattering is dominant over Thomson scattering (TS). This latter was observed but not analyzed. Our observation and analysis are somehow complementary to the one of Thomas *et al.*: in fact, we studied the late propagation of the pulse at intensities, which are definitely sub-relativistic ($a_0 \ll 1$), when Thomson scattered light is the dominant component of side-scattering, while Raman scattering can give only a minor contribution.

We report and discuss here time- and space-resolved observations demonstrating an outstanding, progressive blue shift of the laser spectrum. The process is highly reproducible, regular in time and space. It is then in principle usable for modifying the laser spectrum. It has to be noticed that in the past, most of the spectral studies were performed on the laser pulse getting out from the plasma.^{6–12} This is the most direct way to account for the *total* spectral modification produced by the propagation but this technique does not provide any information on the *dynamic* of the process. Conversely, laser light scattered by the plasma via elastic Thomson scattering can describe the evolution of the spectral changes in *real* time. Imaging Thomson scattered light in laser-plasma interaction studies is quite an usual diagnostics. In our work, we perform a specific spectral study of the laser scattered light. Our experimental conditions guarantee elastic and incoherent Thomson scattering (see Discussion). Our spectra and images give indirect but quantitative information on the spectral evolution of the laser light itself during the pulse propagation. An early work by Sullivan *et al.*¹⁴ is a precursor of our technique. Part of the Sullivan experiment was

^{a)}antonio.giulietti@ino.it. URL: www.ino.it

^{b)}Present address: CELIA-Université Bordeaux, France.

^{c)}Present address: ELI-beamlines, Institute of Physics, Czech Republic.

performed also in nitrogen in conditions not far from ours but the shift observed in the Thomson scattered light was both blue and red and the amount of the blue shift was much smaller than what we observe here. The reason for this difference is that in that early work, the experiment was designed to preserve relativistic intensity as much as possible during propagation; while in our case, de-focusing is allowed to develop and reduce intensity to values for which the self-phase modulation has the maximum effect all over the laser pulse. Another unique feature of our experiment is that we perform high resolution color imaging of the scattering region from which laser spectral changes can be observed with high space- and time-resolution.

A primary role in the nonlinear spectral changes of a laser pulse propagating in a gas at moderate intensity is played by ionization. Though ultrafast laser ionization of the gas is basically a single particle process, collective phenomena, like ultrafast change of the refractive index, may induce non-linear effects on the laser pulse, including de-focusing and spectral upshifting. The latter, in particular, can produce relevant spectral changes. However, also de-focusing¹⁵ has to be carefully considered. At very high laser intensity, in fact, spectral changes due to ionization are negligible: an ultra-intense laser pulse can fully ionize the gas in a time as short as a fraction of a single optical cycle and most of the pulse will propagate in a fully ionized gas with no further ionization nor spectral effects due to ionization. In this regime, other nonlinear mechanisms, nevertheless, can induce spectral changes, like "photon acceleration" mentioned above. At lower intensities, however, when the pulse peak intensity is comparable with threshold intensity for field ionization of the gas, major spectral effects can be induced by phase modulation of the e.m. wave. Our observations indeed correspond to this regime. Basically, self-phase modulation induced by sudden drop of the refractive index results in a blue shift. A number of competitive effects, including further intensity decrease due to either de-focusing or energy depletion of the laser pulse, put a limit to the amount of blue shift $\delta\lambda$. In the present work, such a limit extended up to $\delta\lambda/\lambda \approx 0.4$ in a nitrogen plasma. This is the first time to our knowledge that a shifting process regular in time and

uniform in space along the propagation axis is observed from an initial wavelength of 800 nm down to less than 500 nm at a mean shifting rate of $\approx 3 \text{ \AA}$ per femtosecond. This work can be then a starting point for future research in the field.

II. EXPERIMENT

Our experiment was originally devoted to optimize conditions for electron acceleration in a gas jet at a laser power of 2 TW.¹⁶ In the experiment, a 65-fs duration, 800 nm wavelength, $M^2 \approx 1.5$, 2 TW Ti:Sa CPA laser pulse was focused onto a gas jet with a $f/N \approx 5$ off-axis parabola perpendicularly to the gas flow. Laser polarization was linear and perpendicular to the gas flow as well. Laser bandwidth was $\Delta\lambda = 13 \text{ nm}$. In a 10- μm quasi-Gaussian focal spot, there was a nominal peak intensity of 10^{18} Wcm^{-2} ($a_0 = 0.68$), with a Rayleigh length $L_R = 94 \mu\text{m}$. The high density jet was delivered by a supersonic nozzle¹⁷ with a $1.2 \times 4.0 \text{ mm}$ rectangular slit. The gas jet was irradiated perpendicularly to the 4.0 mm side at about 0.5 mm from the gas jet exit. A variety of mono-atomic or bi-atomic gas species were used in our acceleration experiments and different degrees of ionization were achieved. Spectral changes of the laser pulse were observed in all cases by Thomson diagnostics. In the case of Helium, the observed spectral modification included both red and blue shift with strong modulations. It was mostly attributed to the interplay between self-focused laser light and plasma waves.¹⁸ However, the largest, most regular, and reproducible blue shift was observed in nitrogen. This is likely to be due to the sequence of the first five ionization energies of nitrogen which fit at best the laser intensities for multiphoton (and/or tunnel) ionization during late propagation of our laser pulse in the gas. In the following, we will refer to nitrogen case only.

A layout of the setup is shown in Fig. 1. High charge non-thermal electron bunches (peak kinetic energy of a few MeV) were produced regularly in these conditions^{16,19} and characterized.

However, the most relevant data for this work were given by interferometry and TS diagnostics. The

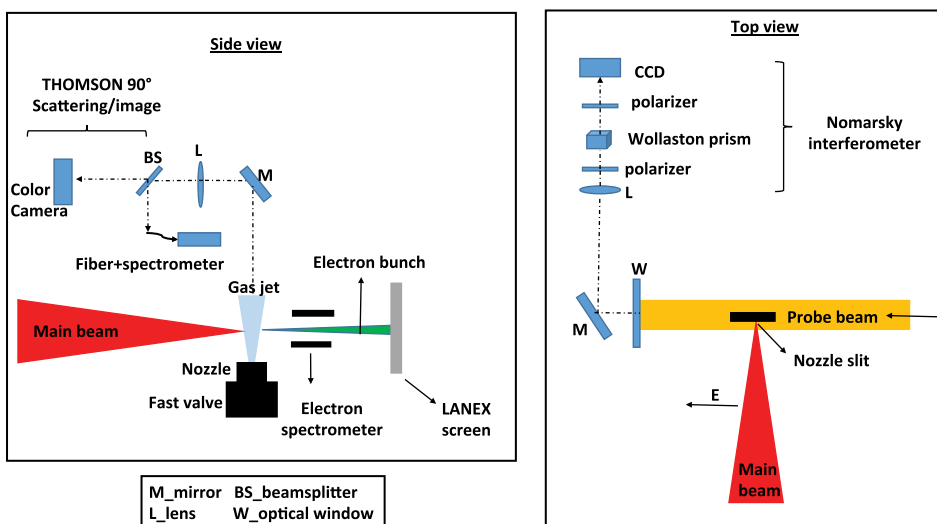


FIG. 1. Layout of the experimental setup both from top- and side-views.

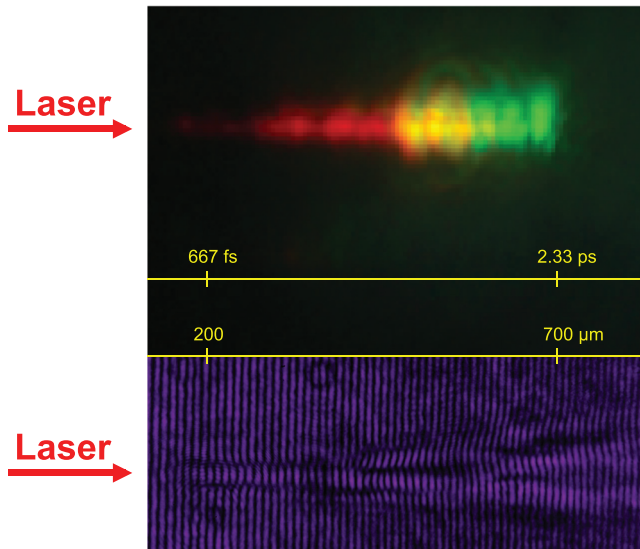


FIG. 2. Top: Color image of the laser-plasma interaction region taken from the Thomson scattered laser light. The laser pulse length is about $20 \mu\text{m}$. The pulse propagates from left to right. The time of transit of the laser pulse is indicated ($t = 0$ is the time of entrance of the pulse in the gas jet). Bottom: Interferogram taken 10 ps after the entrance of the laser pulse in the gas jet. The length of propagation of the pulse is indicated ($x = 0$ at the entrance of the pulse in the gas jet).

interferometer, visible in the top view of Fig. 1, was set in the Nomarski configuration using a separate, frequency doubled “probe” pulse propagating perpendicular to both laser beam and gas-jet flow. Laser light scattered at 90° by Thomson Scattering was collected by an achromatic objective in the direction of gas flow (perpendicular to laser polarization).²⁰ This light was then split in two parts and sent respectively to (a) a spectrally calibrated spectrometer coupled with an optical fiber, allowing a spectral resolution of about 0.8 nm and (b) a color camera CCD array put in the image plane of the objective with magnification $M = 9$. The color camera used to capture images of the scattering sources was a commercial Pentax K100D Super digital camera, which had been previously adapted for single-shot plasma diagnostics, and spectrally calibrated.²¹

As we will discuss below, spectral and spatial information from TS not only provided a useful support to the study of propagation of the laser pulse but also showed unique features of the laser frequency shifting during pulse propagation. Fig. 2 shows two typical data obtained from TS region color imaging (top) and interferometry (bottom), respectively, both displayed on the same spatial scale. In the case of the TS image, also the corresponding time scale of propagation is shown. We recall that the FWHM laser pulse length is of about 65 fs , i.e., $20 \mu\text{m}$ in space. This length roughly corresponds to the minimum longitudinal scale of spectral changes, while the optical resolution given by the objective on the image plane was better than $10 \mu\text{m}$. The color camera image of the scattering region shows three striking features: (a) the regular progressive ultrafast spectral shifting of the TS light along the propagation path from red to yellow, then to green; (b) a sudden, drastic de-focusing occurring in correspondence of the first net color change from red to yellow;

(c) the quasi periodical spatial (i.e., temporal) modulations of the scattered light intensity. All these features were quite reproducible shot-by-shot. As for the spectral changes, it has to be noticed that radially the situation is complicated by the radial distribution of the laser intensity.

The lower part of Fig. 2 shows an interferogram obtained in the same interaction conditions as the image above. It was taken 10 ps after entrance of the laser pulse into the nitrogen gas jet. The laser pulse was focused at the gas-jet front. At the entrance side, the plasma shows a regular cylindrical shape whose length (about $200 \mu\text{m}$) overcomes L_R due to relativistic self focusing and self-guiding.¹⁶ In our regime, relativistic self-focusing has a power threshold of $P_{\text{rsf}} = 17 (n_c/n_e) \text{ GW}$, where n_e and n_c are the local electron density and the critical density, respectively. Neutral nitrogen density and interferograms consistently lead to estimate a peak electron density of $n_e \approx 5 \times 10^{19} \text{ cm}^{-3}$. Consequently, we can evaluate $P_{\text{rsf}} \approx 0.5 \text{ TW}$, easily reached with the 2.0 TW peak power of the laser pulse.¹⁶ Apart from the regular cylindrical region, a complete deconvolution of the interferogram into an electron density map was not possible because of the complicated system of fringes. The shape of the fringe pattern gives however an intuitive idea of the sudden de-focusing of the laser light at about $450 \mu\text{m}$ from laser entrance in the gas. This position corresponds to the laser propagation time of 1.5 ps at which the fast stage of progressive blue shift starts.

Particle in cell numerical simulation performed with both the ALADYN²² and the CALDER code²³ confirm occurrence of relativistic self-focusing and guiding of the laser pulse along a quasi-cylindrical path longer than L_R . Self-focused pulse intensity exceeds $5 \times 10^{18} \text{ W cm}^{-2}$. This high intensity stage is very effective for electron acceleration in a non-linear regime (see also Ref. 24 and simulations therein). In this regime, the laser spectrum can be modified by several processes including “photon acceleration”¹¹ but it is rather insensitive to ionization because laser intensity is too high: only the very leading edge of the pulse is affected by self-phase modulation consequent to ionization. The rest (most) of the pulse passes through the (already) ionized gas without any blue shift. This early regime is represented experimentally in the left part of the image shown in Fig. 2 (top). The electron density left by this initial propagation, as observed 10 ps later, is visible in the left part of the interferogram (Fig. 2—bottom). After this stage dominated by self-focusing of the laser pulse,¹⁶ PIC simulations show substantial energy depletion of the laser pulse, leading to a new regime, dominated by laser ionization, which in turn defocuses the laser pulse. Both depletion and defocusing make the laser intensity drop down to sub-relativistic values close to the ionization thresholds. In this condition, ionization produces a strong ionization-induced frequency up-shift of the laser pulse, as confirmed by TS data. This is also the stage in which Thomson scattering is most effective, as can be seen from the image on top of Fig. 2.

Fig. 3 shows a typical spectrum integrated in space and time of the scattered laser light. The spectrum shows an extraordinary width, mostly on the blue side of the original laser line (centered at 800 nm). The original laser line is

indicated in Fig. 3 by a gray rectangle whose width is equal to the 13 nm FWHM laser line width. Other process beside Thomson scattering can marginally contribute to the spectrum of Fig. 3, mostly at the early stage of propagation in which the intensity is still relativistic or near to ($a_0 \approx 1$) like in the experiment of Thomas *et al.*¹³ where Raman scattering was dominant. In our experimental conditions, Thomson Scattering is the dominant process producing the spectrum collected sideward.

Thomson scattering of a laser pulse by plasma electrons differs from the single electron case. Nevertheless, it has been shown that at laser intensity and plasma density typical of laser driven electron acceleration, Thomson Scattering is elastic and basically linear,²⁵ i.e., the spectrum of local scattering sources is the same as the incoming laser light in that position. In principle, however, interference between electrons can produce *coherent* scattering. This coherent emission can be excluded if the laser wavelength λ_0 is negligible with respect to the Debye length λ_D of the plasma ($\lambda_0 \ll \lambda_D$). For our plasma, we estimate $\lambda_D \approx 10$ nm, which in contrast is much smaller than the laser wavelength, so we may expect coherent scattering. But it turns out²⁶ that emission from single electrons interferes destructively in all directions excluding forwards. Since we detect Thomson Scattering at 90° , we collect the incoherent sum of single-electron emission. Due to the finite transverse extent of the scattering region, the color is however integrated along the line of view. Time-integrated plasma self emission (both continuum and atomic lines) was negligible respect to Thomson scattering. From color image of Fig. 2 (reproducible shot to shot), we can see that shift increases continuously and rather regularly along 300 μm path.

The integrated spectrum shown in Fig. 3 gives instead a quantitative picture of the overall spectral process affecting the laser pulse. The blue limit of the spectrum corresponds to the maximum blue shift which exceeds $\Delta\lambda = -300$ nm at a mean shifting rate of $\delta\lambda/\delta t \approx 3$ Å/fs. Notice that the original laser wavelength appears to be almost suppressed in the spectrum: this surprising effect may be due to the poor

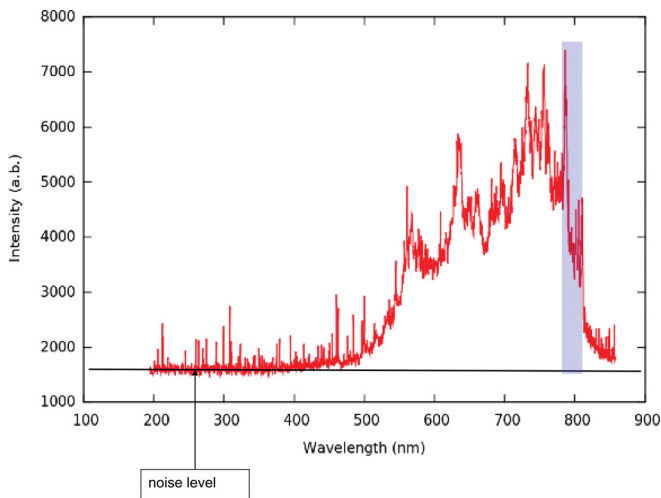


FIG. 3. Spectrum of the scattered laser light, integrated in space and time. The gray rectangle indicates the original laser line.

efficiency of TS at the initial stage of strong self-focusing (small volume and lower density because of ponderomotive electron evacuation). The tiny red-shifted component visible in the spectrum can be attributed to the early, strongly non-linear, stage as due to photon-acceleration-like process. Both red-shifted component and laser peak are merged here in the bright TS blue-shifted component of the spectrum.

III. DISCUSSION AND NUMERICAL SIMULATIONS

Non-linear optics at relativistic intensity has been extensively studied in the past two decades, including spectral effects induced on the laser pulse by its relativistic propagation in a plasma.²⁷ Our observations do not involve relativistic laser intensity and the process can be described with ordinary equations of propagation of an e.m. wave in a medium, which is changing its refractive index during the propagation itself. In many experiments (including this one), the fast change of the refractive index is produced by the same e.m. wave, in a typical self-induced process. In particular, here the fast change is a consequence of a fast ionization of the gas produced by the ultra-short laser pulse. In this sense, the “ionization-induced frequency up-shift” is equivalent to a process of “self phase modulation” of the laser pulse.

The huge blue-shift observed in our experiment is consistent with self-phase modulation of the laser pulse while it ionizes the gas. In general, a variation of the index of refraction $\mu(t)$ produces a shift in the instantaneous phase (self phase modulation) and consequently in its frequency, given by

$$\omega(t) = \frac{d\varphi(t)}{dt} = \omega_0 - \frac{2\pi L}{\lambda_0} \left(\frac{d\mu(t)}{dt} \right),$$

where L is the length of pulse propagation. Consequently, the total change of wavelength can be roughly evaluated^{8,28} as

$$\Delta\lambda = - \frac{e^2 n_i \lambda_0^3 L}{8\pi^2 \epsilon_0 m_e c^3} \frac{dZ}{dt},$$

where $n_i = n_e/Z$ is the ion density. In our case, $Z = 5$ (6th and 7th degree of ionization of nitrogen cannot be reached at our laser intensity) and $L \approx 300$ μm . Assuming $dZ \approx \Delta Z = 5$ and $dt \approx \Delta t = 30$ fs (rising edge duration of the laser pulse), we estimate for the total shift: $\Delta\lambda \approx -360$ nm, which is in a reasonable agreement with the blue limit of the spectrum of Fig. 2.

As for the spatial/temporal modulation of the TS intensity, as shown by Fig. 2 (top), it can be explained in terms of pulsation regime of self-guided propagation.²⁹ In this regime, the scattering efficiency decreases with periodical reduction of the scattering volume and local electron density. It is a typical self-modulation instability. In the limit, $a_0 \ll 1$, as in our case, and disregarding the transverse dynamics, the envelope equation has been calculated analytically.³⁰ This effect has been recently simulated with a numerical code, which reproduces the scale length of the modulations, we observe here.³¹ Also the spectra are modulated quasi periodically. In the

region of the spectrum not far from the original laser line (both in the red and blue side), spectral peaks have a roughly constant separation which could be roughly associated to our plasma density via Raman side-scattering, similar to what reported in Ref. 13. Both spatial and spectral modulations of the scattered light deserve further investigation.

The overall integrated spectrum of Fig. 3 and the color image of Fig. 2 show with impressive evidence the total amount of the blue shift and its growth. However, they remain an indirect observation and do not provide direct measurement for the final spectrum of the pulse. In order to get a quantitative evaluation of the laser spectrum changes during its propagation, we performed *ad hoc* simulations of the process with the numerical CALDER 2D PIC code. A specific version of CALDER has been used in this case, including a “ionization module.”³² The ionization is calculated considering ADK³³ ionization model, neglecting the collisional ionization. The laser pulse is Gaussian with pulse duration of 65 fs. The nominal focused intensity is $3.5 \times 10^{18} \text{ W/cm}^2$, at the entrance of the gas jet, higher than the experimental one to take into account the 2D simulation geometry. The density profile is trapezoidal with a maximum neutral nitrogen density of 10^{19} cm^{-3} on 1 mm length, preceded and followed by linear density ramps of $100 \mu\text{m}$ length.

Fig. 4 reproduces two frames from the simulation of the laser spectrum vs space (time) of propagation. In frame (a), the laser spectrum is obtained at about 0.5 mm after pulse entrance in the gas jet. At this time, the laser intensity is very high due to self-focusing. During this phase, a plasma wave is progressively built which mostly interacts with the front part of the pulse, whereas the rear part sees a chaotic density

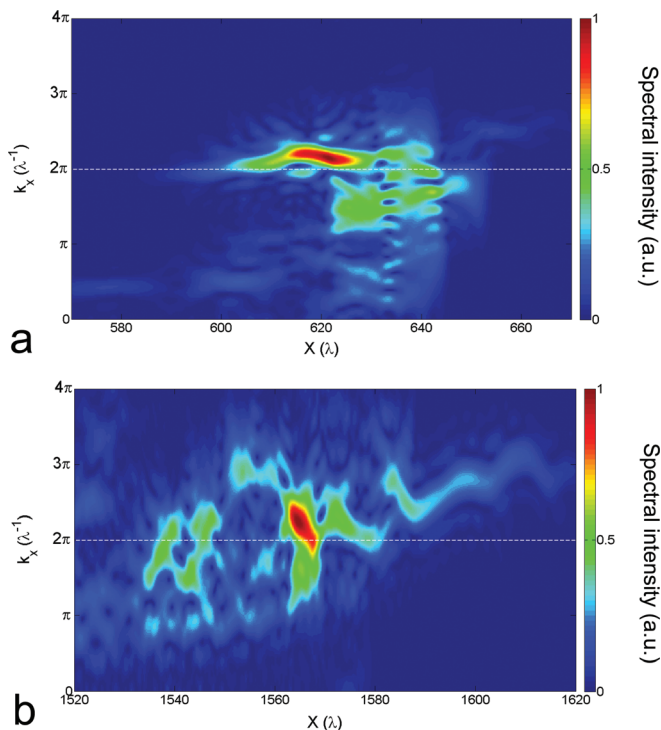


FIG. 4. Spectra of E_y field on axis. For each X_i , the spectrum of the field times a super-Gaussian function, centered on X_i , is given. The wave vector in vacuum k_0 is marked by a white line. (a) 0.5 mm after the pulse entrance in the gas jet and (b) 1.2 mm after entrance.

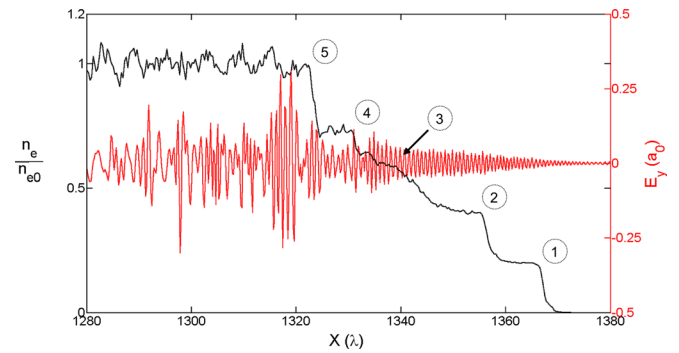


FIG. 5. Electron density (black curve) and E_y field (red curve) on the propagation axis, at 1.0 mm after pulse entrance in the gas jet. Positions of the 5 ionization fronts are indicated.

profile, inducing a slight blue shift. The most intense part of the pulse is already slightly blue shifted, while a less intense part, at the front of the pulse, is red shifted. The red and blue shifts are associated to the modulation of the laser pulse by the plasma. The blue shift of the intense part of the pulse comes from the density gradient. Quantitatively, at this stage, the pulse is slightly shortened (from 65 to 50 fs), blue shifted (from 800 to 740 nm), and spectrally broadened (from 13 to 70 nm). At later times, laser intensity decreases well below 10^{17} Wcm^{-2} and the leading edge of pulse faces an increasing blue shift. This effect dominates the final spectrum of the pulse at its exit from the plasma (1.2 mm after entrance), which is shown in Fig. 4(b). The first part of the pulse is blue shifted, due to gas ionization produced by its front. The second part of the pulse is more affected by the plasma wave, with both red and blue shift. The final balance is that the most intense part of the pulse is mainly blue shifted. Quantitatively, at this stage, the pulse is much shorter (20 fs), the spectrum is peaked at 600 nm and is as broad as 180 nm so extending to about 500 nm, consistent with the integrated spectrum of the scattered light shown in Fig. 3.

To give an idea on how the electron density gradient modifies the laser pulse during its late propagation, we report on Fig. 5 the simulation of electron density profile and the transverse electric field E_y , on axis at an intermediate time. At this time, the peak intensity of the pulse on axis decreased down to $a_0 \approx 0.5$. Electron density increases by steps corresponding to the first 5 ionization degrees. The electron density gradient is responsible for the blue shift.

IV. CONCLUSION

In conclusion, we have observed an extreme blue shift of the laser light, during ultrashort pulse propagation, due to gas ionization by the pulse propagating in nitrogen. The spectral analysis of the laser light scattered during the propagation of an intense ultrashort laser pulse allowed us to follow its spectral evolution in time and space. The huge amount of upshift is consistent with self-phase modulation of the pulse along several hundreds micrometers at an intensity comparable with ionization thresholds. We also observed modulations which can be tentatively attributed to pulsating self-guided propagation but whose deep nature deserves further investigation. Simulations confirm that the laser pulse

spectrum is substantially upshifted by the ionization gradient and supply quantitative description of the pulse evolution in a good agreement with the data provided by Thomson scattering. This agreement is not obvious, also considering that our measurements are performed onto the scattered light, while simulation reproduces directly the spectrum of the laser light itself during propagation. Moreover, simulation was also able to show the evolution of the pulse length, which progressively shorten from 65 to 20 fs due to nonlinear effects occurring during propagation in the dense plasma. Finally, the occurrence of 5-fold ionization of nitrogen is confirmed with clear evidence of the role of the 5 ionization fronts in the process. This work updates a long time research on spectral modification of ultrashort pulses during their propagation in a plasma and brings to a record shift measurement the technique based on Thomson scattering, pioneered by Sullivan *et al.*¹⁴ almost 20 years ago. In addition, the simple but very effective high resolution color imaging method of the scattering region provides a suggestive and realistic view of the ultrafast upshifting of the laser light.

The quite regular and reproducible increase of the blue shift in time and space at a record rate of about 3 Å/fs deserves systematic investigation in view of possible applications, including temporally and spatially resolved diagnostics of ultrafast phenomena, localization of spectrally resonant processes, controlled modification of ultrashort laser pulse spectrum. For this reason, next experiments will be devoted to obtain predictable and reproducible spectral changes of the laser pulse.

ACKNOWLEDGMENTS

This work was supported by the “ELI Italy” funded by CNR and by the γ -RESIST project funded by INFN. Simulation with CALDER code was with HPC resources from GENCI-CCRT/CINES (Grant No. 2011-056067). Deep gratitude is due to Ph. Martin and F. Queré for enlightening discussions. The authors would like to thank also C. A. Cecchetti for his contribution, W. Baldeschi, A. Barbini, F. Pardini, A. Rossi, and M. Voliani for their technical support. A.G. is grateful to Federica Baffigi for her help in revising the manuscript.

¹E. Yablonovitch, *Phys. Rev. A* **10**, 1888 (1974).

²B. P. Corkum, C. Rolland, and T. Srinivasan-rao, *Phys. Rev. Lett.* **57**, 2268 (1986).

³W. M. Wood, C. W. Siders, and M. C. Downers, *Phys. Rev. Lett.* **67**, 3523 (1991).

⁴T. Afshar-rad, S. Coe, A. Giulietti, D. Giulietti, and O. Willi, *Europhys. Lett.* **15**, 745 (1991).

⁵D. Strickland and G. Mourou, *Opt. Commun.* **56**, 219 (1985).

⁶S. P. Le Blanc, R. Sauerbrey, S. C. Rae, and K. Burnett, *J. Opt. Soc. Am. B* **10**, 1801 (1993).

⁷P. R. Bolton, A. B. Bullock, C. D. Decker, M. D. Feit, A. J. P. Megofna, P. E. Young, and D. N. Fittinghoff, *J. Opt. Soc. Am. B* **13**, 336 (1996).

⁸D. Giulietti, L. A. Gizzi, A. Giulietti, A. Macchi, D. Teychenné, P. Chessa, A. Rousse, G. Cherieaux, J. P. Chambaret, and G. Darpentigny, *Phys. Rev. Lett.* **79**, 3194 (1997).

⁹J. K. Koga, N. Naumova, M. Kando, L. N. Tsintsadze, K. Nakajima, S. V. Bulanov, H. Dewa, and H. Kotaki, and T. Tajima, *Phys. Plasmas* **7**, 5223 (2000).

¹⁰A. Giulietti, P. Tomassini, M. Galimberti, D. Giulietti, L. A. Gizzi, P. Koester, L. Labate, T. Ceccotti, P. D’Oliveira, T. Auguste, P. Monot, and Ph. Martin, *Phys. Plasmas* **13**, 093103 (2006).

¹¹C. D. Murphy, R. Trines, J. Vieira, A. J. V. Reitsma, R. Bingham, J. L. Collier, E. J. Divall, P. S. Foster, J. H. Hooker, A. J. Langley, P. A. Norreys, R. A. Fonseca, F. Fiuza, L. O. Silva, J. T. Mendonça, W. B. Mori, J. G. Gallacher, R. Viskup, D. A. Jaroszinski, S. P. D. Mangles, A. G. R. Thomas, K. Krushelnick, and Z. Najmudin, *Phys. Plasmas* **13**, 033108 (2006).

¹²R. M. G. M. Trines, C. D. Murphy, K. L. Lancaster, O. Chekhlov, P. A. Norreys, R. Bingham, J. T. Mendonça, L. O. Silva, S. P. D. Mangles, C. Kamperidis, A. Thomas, K. Krushelnick, and Z. Najmudin, *Plasma Phys. Controlled Fusion* **51**, 024008 (2009).

¹³A. G. R. Thomas, S. P. D. Mangles, Z. Najmudin, M. C. Kaluza, C. D. Murphy, and K. Krushelnick, *Phys. Rev. Lett.* **98**, 054802 (2007).

¹⁴A. Sullivan, H. Hamster, S. P. Gordon, R. W. Falcone, and H. Natel, *Opt. Lett.* **19**, 1544 (1994).

¹⁵T. Auguste, P. Monot, L. A. Lompré, G. Mainfray, and C. Manus, *Opt. Commun.* **89**, 145 (1992).

¹⁶L. A. Gizzi, C. Benedetti, S. Betti, C. A. Cecchetti, A. Gamucci, A. Giulietti, D. Giulietti, P. Koester, L. Labate, T. Levato, F. Michienzi, N. Pathak, A. Sgattoni, G. Turchetti, and F. Vittori, in *Proceedings of the CHANNELING 2008 Conference* (World Sci. Pub., 2010), pp. 495–501; N. C. Pathak, Ph.D. dissertation, University of Pisa, 2011, available at <http://edt.adm.unipi.it/theses/available/edt06272011-134423/>.

¹⁷T. Hosokai, K. Kinoshita, T. Ohkubo, A. Mackawa, and M. Uesaka, *Phys. Rev. E* **73**, 036407 (2006).

¹⁸N. C. Pathak, G. Bussolino, C. A. Cecchetti, A. Giulietti, D. Giulietti, P. Koester, T. Levato, L. Labate, and L. A. Gizzi, *Nucl. Instrum. Methods Phys. Res.* **680**, 103 (2012).

¹⁹N. C. Pathak, C. A. Cecchetti, A. Gamucci, A. Giulietti, D. Giulietti, P. Koester, L. Labate, T. Levato, L. Nizzoli, F. Piastra, and L. A. Gizzi, *Nucl. Instrum. Methods Phys. Res.* **653**, 126 (2011).

²⁰L. A. Gizzi, C. A. Cecchetti, A. Giulietti, D. Giulietti, P. Koester, L. Labate, T. Levato, and N. Pathak, *IEEE Trans. Plasma Sci.* **39**, 2954 (2011).

²¹L. Labate, A. Barbini, L. A. Gizzi, L. M. R. Gartside, and D. Neely, Central Laser Facility Annual Report 2007/2008, UK (2008), p. 276, available at http://www.clf.stfc.ac.uk/resources/PDF/ar07-08_s7_commercial_digital_slr.pdf.

²²C. Benedetti, A. Sgattoni, G. Turchetti, and P. Londrillo, *IEEE Trans. Plasma Sci.* **36**, 1790 (2008).

²³L. Pommier and E. Lefebvre, *Laser Part. Beams* **21**, 573 (2003).

²⁴A. Giulietti, N. Bourgeois, T. Ceccotti, S. Dobosz, P. D’Oliveira, M. Galimberti, J. Galy, A. Gamucci, D. Giulietti, L. A. Gizzi, D. J. Hamilton, E. Lefebvre, L. Labate, J. R. Marquès, P. Monot, H. Popescu, F. Réau, G. Sarri, P. Tomassini, and Ph. Martin, *Phys. Rev. Lett.* **101**, 105002 (2008).

²⁵E. Esarey, S. K. Ride, and P. Sprangle, *Phys. Rev. E* **48**, 3003 (1993).

²⁶S.-Y. Chen, A. Maksimchuk, and D. Umstadter, *Nature* **396**, 653 (1998).

²⁷W. B. Mori, *IEEE J. Quantum Electron.* **33**, 1942 (1997).

²⁸S. C. Rae and K. Burnett, *Phys. Rev. A* **46**, 1084 (1992).

²⁹A. Chiron, G. Bonnaud, A. Dulieu, J. L. Miquel, G. Malka, and M. Louis-Jaquet, *Phys. Plasmas* **3**, 1373 (1996).

³⁰E. Esarey, P. Sprangle, J. Krall, and A. Ting, *IEEE J. Quantum Electron.* **33**, 1879 (1997).

³¹L. Nizzoli, M.S. thesis, University of Pisa, 2010, available at <http://edt.adm.unipi.it/theses/available/edt09292010-102825/>.

³²R. Nuter, L. Gremillet, E. Lefebvre, A. Lévy, T. Ceccotti, and P. Martin, *Phys. Plasmas* **18**, 033107 (2011).

³³M. V. Ammosov, N. B. Delone, and V. P. Krainov, *Sov. Phys. JETP* **64**, 1191 (1986).